

SCIENTIFIC REPORTS

OPEN

Unsaturation of vapour pressure inside leaves of two conifer species

Lucas A. Cernusak¹, Nerea Ubierna², Michael W. Jenkins³, Steven R. Garrity⁴, Thom Rahn⁵, Heath H. Powers⁵, David T. Hanson⁶, Sanna Sevanto⁵, Suan Chin Wong², Nate G. McDowell⁷ & Graham D. Farquhar²

Received: 14 November 2017

Accepted: 30 April 2018

Published online: 16 May 2018

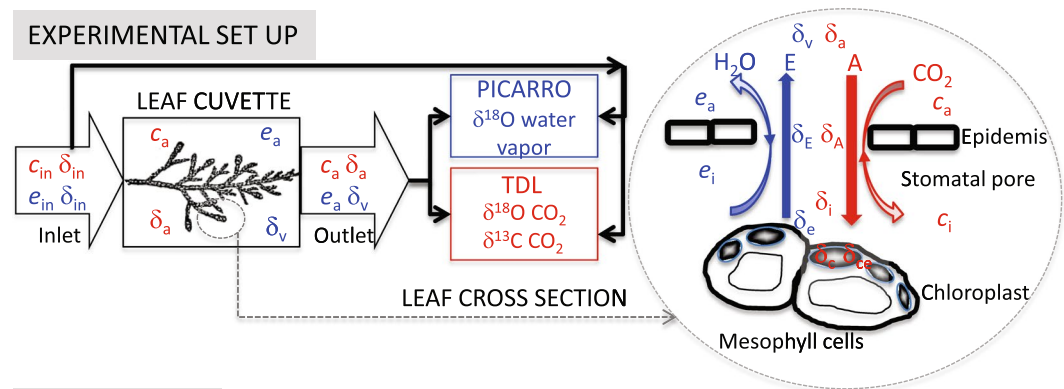
Stomatal conductance (g_s) impacts both photosynthesis and transpiration, and is therefore fundamental to the global carbon and water cycles, food production, and ecosystem services. Mathematical models provide the primary means of analysing this important leaf gas exchange parameter. A nearly universal assumption in such models is that the vapour pressure inside leaves (e_i) remains saturated under all conditions. The validity of this assumption has not been well tested, because so far e_i cannot be measured directly. Here, we test this assumption using a novel technique, based on coupled measurements of leaf gas exchange and the stable isotope compositions of CO_2 and water vapour passing over the leaf. We applied this technique to mature individuals of two semiarid conifer species. In both species, e_i routinely dropped below saturation when leaves were exposed to moderate to high air vapour pressure deficits. Typical values of relative humidity in the intercellular air spaces were as low 0.9 in *Juniperus monosperma* and 0.8 in *Pinus edulis*. These departures of e_i from saturation caused significant biases in calculations of g_s and the intercellular CO_2 concentration. Our results refute the longstanding assumption of saturated vapour pressure in plant leaves under all conditions.

Stomata are microscopic pores that mediate the uptake of CO_2 and loss of water from terrestrial plant leaves¹. Analyses of stomatal function were greatly facilitated by the development of a method for continuous, non-destructive quantification of stomatal conductance (g_s), the Gaastra method². The key to this method is to assume that air inside the leaf is saturated with water vapour, with the saturation vapour pressure (e_s) then calculated according to an exponential relationship with leaf temperature (T_l). With this assumption, g_s can be calculated from measurements of the transpiration rate (E), the vapour pressure of the air outside the leaf (e_a), and T_l , assuming boundary layer conductance (g_b) is known². Furthermore, once g_s has been established, the intercellular CO_2 concentration (c_i) can be calculated^{3,4}. Knowing c_i is useful for relating photosynthetic metabolism and water-use efficiency to environmental conditions. The Gaastra² method of quantifying g_s and c_i has become standard practice in leaf gas exchange studies and is employed in all commercial gas exchange systems.

It has become a dogmatic assumption in the field of plant physiology that the intercellular vapour pressure (e_i) is saturated. If e_i becomes unsaturated under some conditions, this will cause a bias in estimations of g_s and c_i . The vapour pressure inside leaves cannot be measured directly, but in a few studies indirect techniques have been applied to address the question. Results have been mixed, with some authors finding evidence of unsaturation^{5–9}, and others no such evidence^{10–12}; thus, the question has remained unresolved for decades.

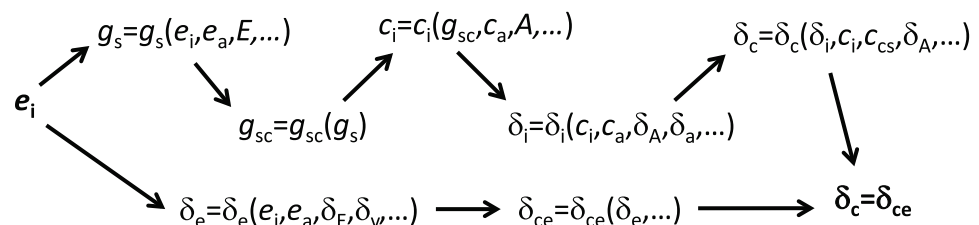
Here we present results from a new type of experiment aimed at quantifying e_i (Fig. 1). The underlying theory and the accompanying system of equations are described in full in the Supplementary Material. As air passes over a C_3 leaf, CO_2 diffuses through the stomata into the intercellular air space, and from there into the chloroplast, where some of it is fixed by RuBisCO. During diffusion through liquid, CO_2 can exchange its oxygen atoms with those in water, with the rate of exchange greatly accelerated by the enzyme carbonic anhydrase. The most relevant site for carbonic anhydrase in this diffusion pathway is thought to be at the chloroplast surface¹³. Of the CO_2 that exchanges its oxygen atoms with water at the chloroplast surface, not all will be fixed by RuBisCO, and some will

¹College of Science and Engineering, James Cook University, Cairns, Queensland, Australia. ²Research School of Biology, The Australian National University, Canberra, Australian Capital Territory, Australia. ³Department of Ecology and Evolutionary Biology, University of California Santa Cruz, California, USA. ⁴METER Group, Inc. Pullman, Washington, USA. ⁵Earth and Environmental Sciences Division, Los Alamos National Laboratory, Los Alamos, New Mexico, USA. ⁶Department of Biology, University of New Mexico, Albuquerque, New Mexico, USA. ⁷Earth Systems Analysis and Modelling Group, Pacific Northwest National Laboratory Richland, Washington, USA. Correspondence and requests for materials should be addressed to L.A.C. (email: lucas.cernusak@jcu.edu.au)



CALCULATIONS

Allow e_i to vary, such that $\delta_c = \delta_{ce}$



SYMBOLS AND ABBREVIATIONS

A	photosynthesis rate	δ_A	$\delta^{18}\text{O}$ of assimilated CO_2
c_a	ambient $[\text{CO}_2]$	δ_a	$\delta^{18}\text{O}$ of ambient CO_2
c_{cs}	chloroplast surface $[\text{CO}_2]$	δ_c	$\delta^{18}\text{O}$ of CO_2 at chloroplast surface
c_i	intercellular $[\text{CO}_2]$	δ_{ce}	$\delta^{18}\text{O}$ of CO_2 in equilibrium with water at chloroplast surface
E	transpiration rate	δ_E	$\delta^{18}\text{O}$ of transpired water
e_a	ambient vapour pressure	δ_e	$\delta^{18}\text{O}$ of evaporative site water
e_i	intercellular vapour pressure	δ_i	$\delta^{18}\text{O}$ of intercellular CO_2
g_s	stomatal conductance to H_2O	δ_v	$\delta^{18}\text{O}$ of ambient water vapour
g_{sc}	stomatal conductance to CO_2		

Figure 1. Experimental design underlying our method for estimating the intercellular vapour pressure, e_i . A twig was placed in the leaf cuvette of a Li-Cor 6400 portable photosynthesis system. The flow of air in and out of the cuvette was split and diverted to water vapour and CO_2 spectroscopic isotope analysers. In the top panel, symbols and fluxes in red relate to CO_2 and those in blue to water vapour. The middle panel shows the basic flow of calculations, and the bottom panel provides definitions for symbols and abbreviations.

diffuse back to the intercellular air space. Therefore, the intercellular air space contains a mixture of CO_2 that has diffused in from the atmosphere carrying $\delta^{18}\text{O}$ signature δ_a , and CO_2 that has diffused back from the chloroplast surface carrying $\delta^{18}\text{O}$ signature δ_c . We use the symbol δ_i to refer to the $\delta^{18}\text{O}$ of this CO_2 mixture in the intercellular air space.

Water at the evaporative sites of leaves becomes enriched in ^{18}O during transpiration¹⁴, with the extent of enrichment described by the well-known Craig-Gordon equation¹⁵. Because chloroplasts are appressed against the cell walls lining the intercellular air spaces in C_3 plants¹⁶, it can be assumed that the $\delta^{18}\text{O}$ of water at the chloroplast surface is very close to that at the evaporative sites¹⁷. The resulting enrichment of ^{18}O in water at the chloroplast surface sets up a catena of enrichment of $\delta^{18}\text{O}$ in CO_2 , with that at the chloroplast surface being highest, that in the intercellular air spaces intermediate, and that in the ambient air lowest. Thus, under typical conditions, we expect to find the pattern, $\delta_c > \delta_i > \delta_a$.

We combined measurements of the oxygen isotope composition of CO_2 entering and exiting a leaf gas exchange cuvette with gas exchange parameters to estimate δ_i . This estimate of δ_i is sensitive to c_i , and is therefore sensitive to g_s , which is in turn sensitive to the assumed value of e_i (Fig. 1). From concurrent measurements of the

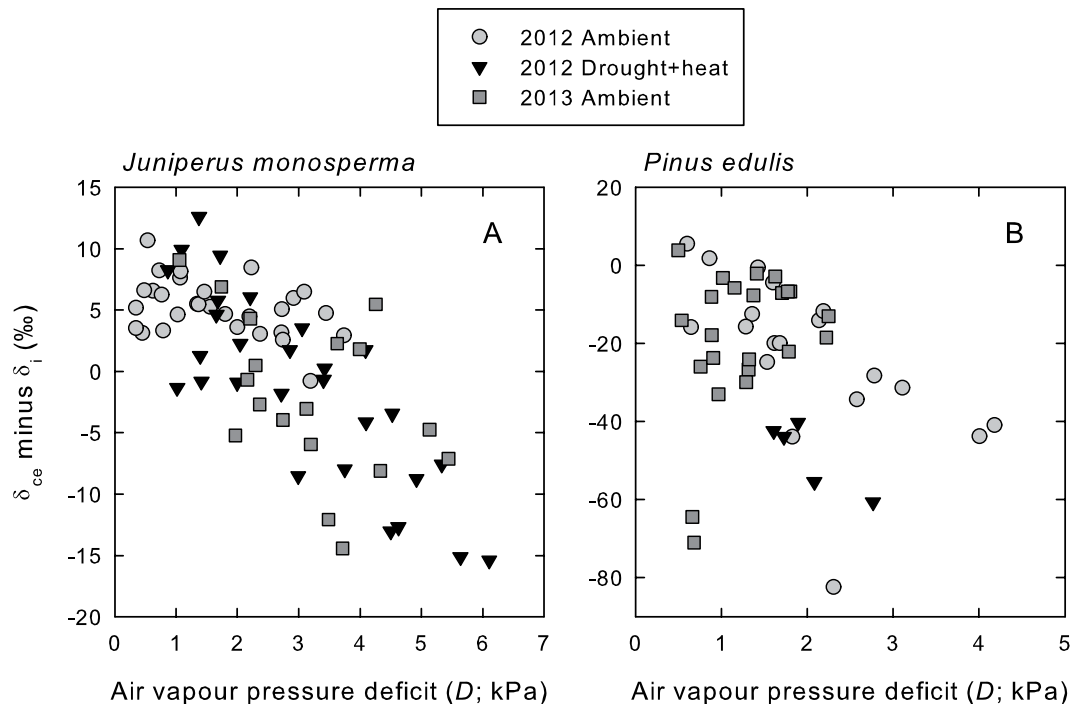


Figure 2. The difference between the $\delta^{18}\text{O}$ of CO_2 in equilibrium with evaporative site water (δ_{ce}) and the $\delta^{18}\text{O}$ of CO_2 in the intercellular air spaces (δ_i) plotted as a function of the air vapour pressure deficit (D) to which the leaf was exposed for *J. monosperma* (A) and *P. edulis* (B). The δ_i and δ_{ce} were calculated assuming saturation of vapour pressure in the intercellular air spaces. Negative values of $\delta_{ce}-\delta_i$ are inconsistent with theoretical expectations in this context, and indicate that the assumption of saturation of intercellular vapour pressure, e_i , was invalid.

$\delta^{18}\text{O}$ of transpired water, we simultaneously estimated $\delta^{18}\text{O}$ of water at the evaporative sites lining the intercellular air spaces (δ_c). The δ_c is also sensitive to the assumed value of e_i , but typically much less so than δ_i . We then calculated the $\delta^{18}\text{O}$ of CO_2 in equilibrium with δ_c , which we term δ_{ce} . Keeping in mind that the true δ_i must reflect a mixture between δ_{ce} and δ_a , we then increased the air vapour pressure deficit (D), to see if the apparent δ_i , calculated by assuming saturated e_i , would remain bounded between δ_{ce} and δ_a . Here and throughout the manuscript we present D as the difference between the saturation vapour pressure at air temperature ($e_{s(T_a)}$) and the air vapour pressure (e_a). We prefer this formulation of D in this context because it provides a description of the evaporative demand of the air outside the leaf which does not depend on an assumed value of e_i .

If δ_i exceeds δ_{ce} when δ_a is well below δ_{ce} , this indicates an error in the calculation of δ_i . Unsaturation of e_i can cause this error. In the next step of our analysis, we solved for the e_i that would be required for δ_c (calculated from δ_i) to be equal to δ_{ce} . This allowed us to quantitatively estimate e_i over a range of D . We used these estimates of e_i to test the longstanding assumption that the vapour pressure of air inside leaves remains saturated even as the evaporative demand of the air outside the leaf increases.

Results and Discussion

The δ_a in our experiment, measured in the gas stream exiting the gas exchange cuvette, ranged from 12 to 27‰ (VSMOW). The δ_{ce} ranged from 40 to 68‰ for *J. monosperma* and from 52 to 71‰ for *P. edulis*. Thus, as expected, δ_{ce} was always substantially higher than δ_a . As described above, theory dictates that δ_i should lie between δ_a and δ_{ce} . However, as D increased in the cuvette, we observed that the apparent δ_i became larger than δ_{ce} , such that the difference between δ_{ce} and δ_i became negative in both species (Fig. 2). Calculation of both parameters assumed saturation of e_i . The increasingly negative values of $\delta_{ce}-\delta_i$ with increasing D indicate errors in the estimation of δ_i under high D ; these errors can be reconciled by allowing e_i to drop below saturation as D increased.

Are there other possible explanations for δ_i becoming larger than δ_{ce} at moderate to high D ? We considered five possible alternative explanations: (1) decreasing effectiveness of carbonic anhydrase with decreasing leaf water potential, such that the $\delta^{18}\text{O}$ of CO_2 at the chloroplast surface might not be completely equilibrated with local water; (2) somewhat less ^{18}O -enriched water at the chloroplast surface than that at the evaporative sites due to a Péclet effect¹⁸; (3) a fractionation factor for static diffusion of H_2^{18}O through the stomatal pore of 32‰ rather than 28‰^{19–21}; (4) an error associated with neglecting cuticular conductance in gas exchange calculations^{22,23}; and (5) a bias in the measurement of T_1 by the energy balance method. These possible alternative explanations are addressed in full in the Supplementary Material. In summary, none of them can account satisfactorily for observations of δ_i surpassing δ_{ce} . Therefore, the most likely explanation remains that e_i declined below saturation as D increased.

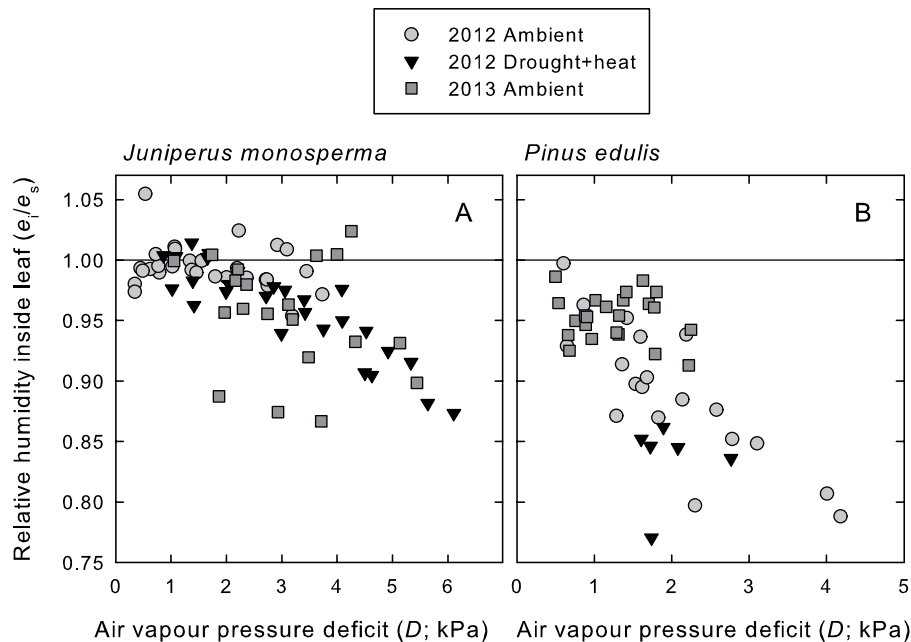


Figure 3. Relative humidity in the intercellular air spaces inside the leaves of two semiarid conifer species plotted as a function of the air vapour pressure deficit (D) to which the leaves were exposed in the gas exchange cuvette for *J. monosperma* (A) and *P. edulis* (B). The relative humidity is defined as e_i/e_s , where e_i is the intercellular vapour pressure and e_s is the saturation vapour pressure at leaf temperature. A relative humidity of unity indicates saturation, and is denoted by the horizontal line within each panel. The analysis demonstrates clear evidence of unsaturation of the internal humidity, even at rather modest air vapour pressure deficits, for these semiarid conifers. A segmented regression analysis indicated a breakpoint in the regression for *J. monosperma* at air vapour pressure deficit of 1.6 kPa, below which the slope was not significant. Above 1.6 kPa for *J. monosperma*, the slope was estimated to be -0.021 kPa^{-1} ($R^2 = 0.35$, $P < 0.0001$, $n = 54$). For *P. edulis*, no breakpoint was identified, and a slope of -0.049 kPa^{-1} was estimated ($R^2 = 0.49$, $P < 0.0001$, $n = 48$).

Next, we solved for the e_i required for δ_c , the $\delta^{18}\text{O}$ of CO_2 at the chloroplast surface calculated from δ_p , to be equal to δ_{ce} , the $\delta^{18}\text{O}$ of CO_2 at the chloroplast surface calculated from δ_c . This allowed us to quantitatively estimate e_i . This calculation required an estimate of g_{mc} , the conductance to CO_2 from the intercellular air space to the site of carbonic anhydrase activity. We inferred values of g_{mc} such that they resulted in estimates of e_i near to saturation when D was lowest. Estimates of the relative humidity inside the leaf made by assuming these values of g_{mc} are shown in Fig. 3. These estimates decreased as D increased in both species, declining to values in the range of 0.9 in *J. monosperma* and 0.8 in *P. edulis*. As a result of these departures of e_i from saturation, our analysis indicated that c_i could be underestimated by as much as $80 \mu\text{mol mol}^{-1}$, and g_s by as much as $30 \text{ mmol m}^{-2} \text{ s}^{-1}$ (Fig. 4).

To demonstrate the impact of choosing different values for g_{mc} , we conducted a sensitivity analysis, in which we calculated the relative humidity inside the leaf (e_i/e_s) for values of g_{mc} twice those originally assigned and for values half those originally assigned. These estimates of e_i/e_s are shown in Supplementary Figure 1. From this figure, one can see that doubling the assigned g_{mc} shifted the range of e_i/e_s estimates up, and halving it shifted the range of e_i/e_s estimates down. However the shifts were not so large as to substantially alter our interpretation of the results. Thus, while it is clear that estimates of e_i/e_s by our technique are sensitive to assigned values of g_{mc} , they are not hypersensitive, and our conclusion that e_i/e_s declined well below unity at moderate to high D would hold for any of the three parameterisations shown in Fig. 3 and Supplementary Figure 1.

Our observations of unsaturation of e_i at moderate to high D are in agreement with recent results from an experiment with angiosperm species *Gossypium hirsutum* and *Eucalyptus pauciflora* (Wong, Canny and Farquhar, unpublished). In that experiment, gas exchange was measured independently on upper and lower leaf surfaces, with the lower leaf surface exposed to air with CO_2 concentration reduced so that net photosynthetic rate was zero, and the upper leaf surface to air with CO_2 concentration near the ambient atmospheric value. Under such conditions, a gradient of c_i should have existed from the upper to the lower surface. As D increased above about 2 kPa, the apparent c_i gradient reversed, indicating that the calculations of c_i were in error; the most parsimonious explanation was unsaturation of e_i .

In our experiment, *P. edulis* showed a stronger tendency toward unsaturation of e_i with increasing D than did *J. monosperma*. The two species are known to differ in their hydraulic behaviour: *P. edulis* is relatively isohydric, whereas *J. monosperma* is relatively anisohydric^{24,25}; stem hydraulic conductivity decreases more strongly in response to decreasing soil water potential in *P. edulis* than in *J. monosperma*²⁶; and the bulk modulus of elasticity is lower in *P. edulis* than in *J. monosperma* leaf tissue²⁵, suggesting mesophyll cell wall function differs between the two species. Our data suggest a coordination in hydraulic behaviour between the stem xylem and the mesophyll cell walls. As the evaporation rate from the mesophyll cell walls increased in response to increasing D , stronger flexure of the meniscus

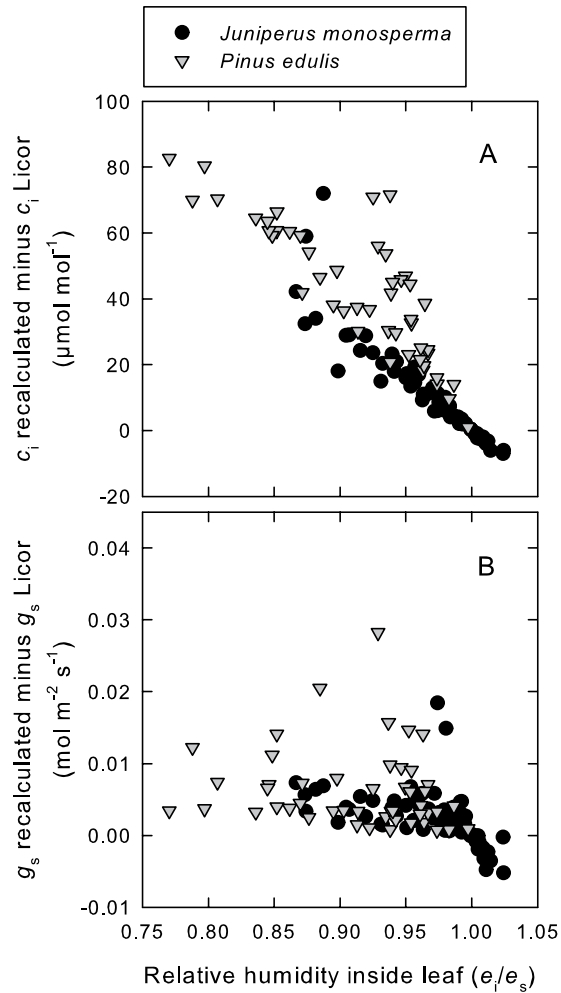


Figure 4. The difference between the intercellular CO₂ concentration (c_i) calculated without assuming saturation of intercellular vapour pressure (e_i) and that calculated by the Li-Cor portable photosynthesis system assuming saturation of e_i (A) and the difference between stomatal conductance (g_s) calculated without assuming saturation of e_i and that calculated by the Li-Cor portable photosynthesis system assuming saturation of e_i (B) plotted against the relative humidity in the intercellular air spaces. The relative humidity inside the leaf on the x-axis was generated from calculations that did not assume saturation of e_i .

in the cell wall pores would have decreased the cross sectional area of pore space, causing an increase in frictional resistance to water movement, and therefore a reduction in mesophyll cell wall hydraulic conductivity²⁷. Our results suggested a steeper decline in mesophyll cell wall hydraulic conductivity in *P. edulis* than in *J. monosperma* as D increased, analogous to steeper declines in xylem hydraulic conductivity with decreasing water availability.

Here we provide the first experimental evidence of unsaturation of e_i in conifer trees by applying a novel method to estimate e_i under field conditions. There are few previous reports of unsaturation of e_i , likely because there is no simple method for directly measuring e_i . Recent theoretical treatments differ in their assertions as to the importance of unsaturation of e_i for leaf gas exchange^{28,29}. We show here that the potential errors that can occur in the estimation of g_s and c_i by assuming saturation of e_i can be significant. Leaf gas exchange measurements are globally common, and errors associated with assuming saturation of e_i could have a major impact on their interpretation. Our method of determining e_i has potential for broad application, given recent technological advances in laser-based methods for determining $\delta^{18}\text{O}$ of CO₂ and water vapour³⁰. This could open the door to new insights into how leaves regulate water loss, with fundamental implications for understanding environmental constraints on plant function.

Methods

Our experiment took place at Los Alamos National Laboratory's Survival-Mortality (SUMO) outdoor experiment (35.8180°N, 106.3053°E, elevation 2180 m). The soil texture at the site is sandy loam at the surface grading to a clay loam with depth^{31,32}. Soil depth ranges from 40 to 80 cm. The site is located in an upland topographic position near the ecotone between piñon-juniper woodland and ponderosa pine forest. *Pinus edulis* and *Juniperus monosperma* are the dominant tree species. The 30 year mean annual temperature and precipitation at a meteorological tower located about 1 km from the site are 9.2 °C and 470 mm, respectively. Roughly half of the annual total precipitation falls from July to September during the North American Monsoon.

For this study, we used mature trees of both species, located within and on the periphery of the SUMO experiment. The experiment comprises control, drought and heat treatments designed to mimic historic conditions during mortality-inducing drought in piñon-juniper woodlands³³ and during extreme heat waves. The control trees were growing in ambient temperature and precipitation with no experimental manipulation; and the treated trees were exposed to ~50% precipitation reduction by rainfall exclusion and ~5 °C above ambient temperature by open-top chambers³⁴. The rainfall exclusion structure was installed on 1 June 2012 and heat treatments were operational on 11 June 2012³⁵.

Our measurements took place from 11–24 September 2012 and from 23–30 August 2013, and included individuals of both *J. monosperma* and *P. edulis*. Control trees of both species were measured in both campaigns and drought + heat trees were measured during the 2012 campaign. Ambient conditions were drier during the 2013 campaign and gas exchange rates in drought + heat trees were too low for measurements at that time, so the 2013 campaign included only un-manipulated control trees.

We coupled a Tunable Diode Laser (TDL; TGA100A, Campbell Scientific Inc., Logan, UT, USA) to a portable photosynthesis system (Li-Cor 6400; Li-Cor Biosciences, Lincoln, NE, USA) fitted with a conifer cuvette (Li-Cor 6400-22) to quantify the concentration of CO₂ and its isotopic composition ($\delta^{13}\text{C}$ and $\delta^{18}\text{O}$) in gas entering and exiting the leaf chamber. The gas streams were plumbed directly into the TDL using ultra-low porosity tubing (Synflex type 1300 1/4 in diameter; Saint Gobain Performance Plastics, Northboro, MA, USA). The TDL data acquisition and processing were as described previously³⁶.

Calibration of the TDL was maintained by using two working standard (WS) calibration tanks during measurements. These WS tanks were calibrated against World Meteorological Organization (WMO) certified standard tanks. To account for instrument drift, the TDL measured the high and low WS tanks during a 3 min cycle also including measurements of the gas exchange cuvette inlet and outlet gas streams. For each 3 min cycle, we calculated the deviation between the measured values and the known values to determine a gain and offset for each isotopologue³⁷. These gain and offset values were then applied to all data in the 3 min measurement cycle. The measurements of gas entering and exiting the cuvette fell within the range of isotopologue concentrations within the two WS tanks.

Before the gas streams entered the TDL, part of the flow was diverted to a cavity-ring-down spectroscopy water isotope analyser (Picarro L2130-i, Picarro Inc., Santa Clara, CA, USA) that measured the $\delta^{18}\text{O}$ of water vapour. The pre- and post-cuvette gas streams were measured for 10 min each at approximately 1 Hz, and the final 5 min of measurements was averaged for each gas stream. The water isotope analyser was calibrated with WS waters. These were introduced into the analyser either using the associated vaporizer unit or by sampling air from sealed plastic bags equilibrated with WS water samples enclosed within them. The temperature dependent liquid-vapour equilibrium fractionation factor was applied in the latter case. The WS water vapours were run once per day.

Our sampling regime was designed to loosely mimic the increasing D that a leaf typically experiences from early morning through to the afternoon. For the most part, we measured one foliage sample per day. The terminal part of a *J. monosperma* or *P. edulis* twig was placed in the Licor conifer chamber one to two hours after sunrise. The entry point of the twig into the cuvette and all exposed gasket surfaces were covered with flexible putty (Terostat IX, Henkel Technologies, Düsseldorf, Germany) to minimize diffusion leaks. The first measurement generally took place under irradiance of 300 $\mu\text{mol photons m}^{-2} \text{s}^{-1}$, and at T_l between 15 and 20 °C. The leaves were allowed to stabilise their gas exchange in the cuvette for about 30 min before a measurement began. Thereafter, we recorded gas exchange, $\delta^{18}\text{O}$ of CO₂ and $\delta^{18}\text{O}$ of water vapour for 20 min. The irradiance and cuvette temperature were then increased, such that a series of measurements was made for each foliage sample from low to high D . The range of T_l in the dataset was from 14.6 to 40.8 °C, and the range of photosynthetically active radiation from 300 to 2200 $\mu\text{mol photons m}^{-2} \text{s}^{-1}$. Chamber flow rate was varied between 250 and 500 $\mu\text{mol s}^{-1}$, with the aim of maintaining a [CO₂] drawdown in the leaf chamber of at least 15 $\mu\text{mol mol}^{-1}$. The [CO₂] within the chamber was approximately 390 $\mu\text{mol mol}^{-1}$. The series of measurements for each foliage sample usually continued until gas exchange diminished as a result of high D to such an extent that a 15 $\mu\text{mol mol}^{-1}$ [CO₂] drawdown between chamber inlet and outlet could not be achieved.

All gas exchange and isotopic calculations are described in detail in the Supplementary Material. Segmented regression analysis was performed using SegReg freeware (<https://www.waterlog.info/segreg.htm>), and all other regression analyses were performed in Systat 12 (Systat Software Inc., San Jose, CA, USA).

Data availability. The datasets generated and analysed during the current study are available from the corresponding author on reasonable request.

References

- Farquhar, G. D. & Sharkey, T. D. Stomatal conductance and photosynthesis. *Annu. Rev. Plant Physiol.* **33**, 317–345 (1982).
- Gaastera, P. Photosynthesis of crop plants as influenced by light, carbon dioxide, temperature and stomatal diffusion resistance. *Meded. Landbouwhogeschool, Wageningen* **59**, 1–68 (1959).
- Moss, D. N. & Rawlins, S. L. Concentration of carbon dioxide inside leaves. *Nature* **197**, 1320–1321 (1963).
- von Caemmerer, S. & Farquhar, G. D. Some relationships between the biochemistry of photosynthesis and the gas exchange of leaves. *Planta* **153**, 376–387 (1981).
- Canny, M. J. & Huang, C. X. Leaf water content and palisade cell size. *New Phyt.* **170**, 75–85 (2006).
- Jarvis, P. G. & Slatyer, R. O. The role of the mesophyll cell wall in leaf transpiration. *Planta* **90**, 303–322 (1970).
- Ward, D. A. & Bunce, J. A. Novel evidence for a lack of water-vapor saturation within the intercellular airspace of turgid leaves of mesophytic species. *J. Exp. Bot.* **37**, 504–516 (1986).
- Karpushkin, L. T. A compensation gasometric method for estimating the kinetic parameters of H₂O and CO₂ exchange in plant leaves. *Russ. J. Plant Physiol.* **41**, 410–413 (1994).
- Egorov, V. P. & Karpushkin, L. T. Determination of air humidity over evaporating surface inside a leaf by a compensation method. *Photosynthetica* **22**, 394–404 (1988).
- Farquhar, G. D. & Raschke, K. On the resistance to transpiration of sites of evaporation within leaf. *Plant Physiol.* **61**, 1000–1005 (1978).
- Jones, H. G. & Higgs, K. H. Resistance to water loss from mesophyll cell surface in plant leaves. *J. Exp. Bot.* **31**, 545–553 (1980).

12. Sharkey, T. D., Imai, K., Farquhar, G. D. & Cowan, I. R. A direct confirmation of the standard method of estimating inter-cellular partial-pressure of CO₂. *Plant Physiol.* **69**, 657–659 (1982).
13. Gillon, J. S. & Yakir, D. Internal conductance to CO₂ diffusion and C¹⁸O discrimination in C₃ leaves. *Plant Physiol.* **123**, 201–213 (2000).
14. Cernusak, L. A. *et al.* Stable isotopes in leaf water of terrestrial plants. *Plant Cell Environ.* **39**, 1087–1102 (2016).
15. Craig, H. & Gordon, L. I. In *Proceedings of a Conference on Stable Isotopes in Oceanographic Studies and Palaeotemperatures* (ed. Tongiorgi, E.) 9–130 (Lischi and Figli, 1965).
16. Busch, F. A., Sage, T. L., Cousins, A. B. & Sage, R. F. C₃ plants enhance rates of photosynthesis by reassimilating photorespired and respired CO₂. *Plant Cell Environ.* **36**, 200–212 (2013).
17. Farquhar, G. D. *et al.* Vegetation effects on the isotope composition of oxygen in atmospheric CO₂. *Nature* **363**, 439–443 (1993).
18. Farquhar, G. D. & Lloyd, J. In *Stable Isotopes and Plant Carbon-Water Relations* (eds Ehleringer, J. R. Hall, A. E. & Farquhar, G. D.) 47–70 (Academic Press, 1993).
19. Cappa, C. D., Hendricks, M. B., DePaulo, D. J. & Cohen, R. C. Isotopic fractionation of water during evaporation. *J. Geophys. Res.* **108**, 4525 (2003).
20. Luz, B., Barkan, E., Yam, R. & Shemesh, A. Fractionation of oxygen and hydrogen isotopes in evaporating water. *Geochim. Cosmochim. Acta* **73**, 6697–6703 (2009).
21. Merlivat, L. Molecular diffusivities of H₂¹⁶O, HD¹⁶O, and H₂¹⁸O in gases. *J. Chem. Phys.* **69**, 2864–2871 (1978).
22. Boyer, J. S. Turgor and the transport of CO₂ and water across the cuticle (epidermis) of leaves. *J. Exp. Bot.* **66**, 2625–2633 (2015).
23. Hanson, D. T., Stutz, S. S. & Boyer, J. S. Why small fluxes matter: the case and approaches for improving measurements of photosynthesis and (photo)respiration. *J. Exp. Bot.* **67**, 3027–3039 (2016).
24. McDowell, N. *et al.* Mechanisms of plant survival and mortality during drought: why do some plants survive while others succumb to drought? *New Phyt.* **178**, 719–739 (2008).
25. Meinzer, F. C., Woodruff, D. R., Marias, D. E., McCulloh, K. A. & Sevanto, S. Dynamics of leaf water relations components in co-occurring iso- and anisohydric conifer species. *Plant Cell Environ.* **37**, 2577–2586 (2014).
26. Pangle, R. E. *et al.* Prolonged experimental drought reduces plant hydraulic conductance and transpiration and increases mortality in a piñon-juniper woodland. *Ecol. Evol.* **5**, 1618–1638 (2015).
27. Egorov, V. P. & Karpushkin, L. T. Experimental investigation and modeling of the interrelationship between kinetic parameters of leaf water exchange. *Sov. Plant Physiol.* **37**, 842–850 (1990).
28. Buckley, T. N., John, G. P., Scoffoni, C. & Sack, L. The sites of evaporation within leaves. *Plant Physiol.* **173**, 1763–1782 (2017).
29. Vesala, T. *et al.* Effect of leaf water potential on internal humidity and CO₂ dissolution: reverse transpiration and improved water use efficiency under negative pressure. *Front. Plant Sci.* **8** (2017).
30. Griffis, T. J. Tracing the flow of carbon dioxide and water vapor between the biosphere and atmosphere: A review of optical isotope techniques and their application. *Ag. For. Met* **174**, 85–109 (2013).
31. Breshears, D. D., Myers, O. B. & Barnes, F. J. Horizontal heterogeneity in the frequency of plant-available water with woodland intercanopy-canopy vegetation patch type rivals that occurring vertically by soil depth. *Ecohydrology* **2**, 503–519 (2009).
32. Davenport, D. W., Wilcox, B. P. & Breshears, D. D. Soil morphology of canopy and intercanopy sites in a piñon-juniper woodland. *Soil Sci. Soc. Am. J.* **60**, 1881–1887 (1996).
33. Breshears, D. D. *et al.* Regional vegetation die-off in response to global-change-type drought. *Proc. Natl. Acad. Sci. USA* **102**, 15144–15148 (2005).
34. Adams, H. D. *et al.* Experimental drought and heat can delay phenological development and reduce foliar and shoot growth in semiarid trees. *Global Change Biol.* **21**, 4210–4220 (2015).
35. Garcia-Forner, N. *et al.* Responses of two semiarid conifer tree species to reduced precipitation and warming reveal new perspectives for stomatal regulation. *Plant Cell Environ.* **39**, 38–49 (2016).
36. Bickford, C. P., McDowell, N. G., Erhardt, E. B. & Hanson, D. T. High-frequency field measurements of diurnal carbon isotope discrimination and internal conductance in a semi-arid species, *Juniperus monosperma*. *Plant Cell Environ.* **32**, 796–810 (2009).
37. Bowling, D. R., Sargent, S. D., Tanner, B. D. & Ehleringer, J. R. Tunable diode laser absorption spectroscopy for stable isotope studies of ecosystem-atmosphere CO₂ exchange. *Ag. For. Met.* **118**, 1–19 (2003).

Acknowledgements

We thank Meisha Holloway-Phillips, Alex Cheesman, Hilary Stuart-Williams, and Michael Roderick for helpful discussions and comments on the manuscript; and Lily Cohen, Adam Collins, and Turin Dickman for measurement and field assistance. This research was supported by Australian Research Council Discovery Grants DP1097276 and DP150100588.

Author Contributions

L.A.C., N.U., M.W.J., S.R.G., T.R., H.H.P., D.T.H., S.S. and N.G.M. contributed to equipment setup and field measurements. L.A.C., N.U., S.C.W. and G.D.F. developed the theoretical approach. L.A.C. and N.U. performed analysis and calculations for figures and results which appear in the text. L.A.C. wrote the first draft, and all authors contributed to the final draft.

Additional Information

Supplementary information accompanies this paper at <https://doi.org/10.1038/s41598-018-25838-2>.

Competing Interests: The authors declare no competing interests.

Publisher's note: Springer Nature remains neutral with regard to jurisdictional claims in published maps and institutional affiliations.



Open Access This article is licensed under a Creative Commons Attribution 4.0 International License, which permits use, sharing, adaptation, distribution and reproduction in any medium or format, as long as you give appropriate credit to the original author(s) and the source, provide a link to the Creative Commons license, and indicate if changes were made. The images or other third party material in this article are included in the article's Creative Commons license, unless indicated otherwise in a credit line to the material. If material is not included in the article's Creative Commons license and your intended use is not permitted by statutory regulation or exceeds the permitted use, you will need to obtain permission directly from the copyright holder. To view a copy of this license, visit <http://creativecommons.org/licenses/by/4.0/>.

© The Author(s) 2018